《연구논문》 Korean Journal of Optics and Photonics, Vol. 29, No. 1, February 2018, pp. 32-39
DOI: https://doi.org/10.3807/KJOP.2018.29.1.032
ISSN : 1225-6285(Print)
ISSN : 2287-321X(Online)

Effect of Amplified Spontaneous Emission on the Gain Recovery of a Semiconductor Optical Amplifier

Hojoon Lee†

Department of Information Communication Engineering, Hoseo University, 20, Hoseo-ro 79beon-gil, Baebang-eup, Asan 31499, Korea

(Received December 7, 2017; Revised January 22, 2018; Accepted January 25, 2018)

The impact of the amplified spontaneous emission (ASE) on the gain recovery time of a bulk semiconductor optical amplifier (SOA) is investigated. The gain-recovery time is obtained by determining the time evolution of the gain, carrier density, and ASE in an SOA, after the propagation of a short pump pulse and continuous-wave (CW) probe of gain dynamics. In the simulation, a wide-band-semiconductor model, which can be characterized by the material gain coefficient over a wide wavelength range, is used, because the gain bandwidth of a practical SOA is very wide. The pump pulse and counterpropagating CW probe field are considered in the simulation, with the ASE noise spectrum equally divided.

Keywords: Amplified spontaneous emission (ASE), Semiconductor optical amplifiers (SOA), Gain recovery time
OCIS codes: (250.5980) Semiconductor optical amplifiers; (250.6715) Switching; (140.3280) Laser amplifiers; (230.4480) Optical amplifiers

I. Introduction

Dense wavelength-division multiplexing (DWDM) fully exploits the available bandwidth of an optical fiber, and an optical-fiber amplifier is used to compensate the optical fiber's losses. All-optical signal processing, such as 2R (reamplification and reshaping) or 3R (reamplification, reshaping, and retiming) regeneration, wavelength switching, and optical time-division multiplexing, draws attention nowadays. The fundamental nonlinearity comes from gain saturation when the CW probe laser and pulsed pump laser are propagating in the SOA. The gain-saturation effect in an SOA is used in optical signal processing gates, by means of cross-gain modulation (XGM) or cross-phase modulation (XPM)[1]. The gain recovery of an SOA occurs on two different time scales. The first, on the scale of 1 ps, results from intraband effects such as spectral hole burning, carrier heating, and two-photon absorption. The other, on the order of 10 ps to 1 ns, results from the time it takes for a conventional SOA to achieve carrier-density inversion, which is limited by long carrier lifetimes. Only the latter is considered in this paper.

The gain-recovery dynamics of an SOA, including the effect of ASE, is investigated, to explain the gain overshoot that can be observed in the temporal dynamics of SOA gain after the crossing of a short saturating pump pulse[2]. Reduced gain-recovery time can be obtained by increasing the applied current, or the physical length of the device. However, these methods have some drawbacks and side effects, such as narrowing of the gain bandwidth, and an increase in ASE. To overcome these problems, research using a CW holding beam, to maintain the separation of the quasi-Fermi levels and enhance the recovery rate, has been reported. The gain-recovery time of an SOA can be reduced using a CW pump laser, so that the pattern effect occuring at high bit rates can be removed[3,4]. Even a large amount of probe gain is reduced when the CW pump is in the gain region. The use of an assisting beam at the transparency wavelength of the SOA can yield very fast operation without reduction of the available gain[5,6]. Those results confirm the feasibility of enhancing SOA recovery rate by CW pump light near the material transparency wavelength[7]. Recently, the effects of CW probe wavelength on gain recovery, SOA device length, and carrier density associated with interband recombination process in quantum wells were measured experimentally, with numerical simulation showing good agreement[8].

In this paper, the impact of ASE on the gain-recovery time of a bulk SOA is investigated. The gain-recovery time is obtained by determining the time evolution of the gain, carrier density, and ASE in an SOA, after the propagation of a short pump pulse and CW probe of the gain dynamics. In

†E-mail: hojoon@hoseo.edu, ORCID: 0000-0002-3423-6025
Color versions of one or more of the figures in this paper are available online.

the simulation, a wideband-semiconductor model[9], which can be characterized by the material gain coefficient over a wide wavelength range, is used, because the gain bandwidth of a practical SOA is very wide. The pump pulse and CW probe field propagating both forward and backward are considered in the simulation, with the ASE noise spectrum equally divided in N_s. The paper is organized as follows: In Section II, we describe the field transmission equations, rate equation, and boundary conditions that govern the model of the SOA, and the wideband model that describes the material gain and spontaneous emission rate of the SOA. In Section III, computer simulations of the time evolution of the output probe waveform are performed, to obtain the gain-recovery times for several cases. For the cases without and with ASE, the change in gain-recovery time is explained. Finally, we conclude the paper in Section IV.

II. Theoretical Model and Laser Parameters

2.1. Modeling the Semiconductor Optical Amplifier

To investigate the gain compression and recovery times of semiconductor optical amplifier (SOA), the pump-probe configuration shown in Fig. 1 is considered. A low-power CW probe laser with a wavelength tunable between 1450 and 1600 nm is assumed in the calculation. The probe is launched into the right side of the SOA. The pump laser that counter-propagates with respect to the probe laser has a short pulse width of 10 ps and a wavelength of 1550 nm. The energy of the pump pulse from 1 pJ to 1 fJ, which can saturate the SOA.

We consider a model SOA with an InP-$In_{1-x}Ga_xAs_yP_{1-y}$ homogeneous buried ridge stripe structure, operating at 1550 nm[10]. The active region and waveguide section of the SOA consist of width W, thickness d, and length L, and are surrounded by InP. The fraction of the pump power actually coupled to the active region is governed by the optical confinement factor Γ. The facet reflectivities of the SOA are

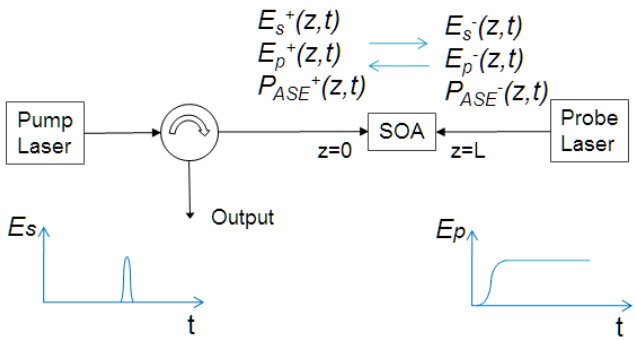

Fig. 1. Schematic for measuring the gain-recovery time of a semiconductor optical amplifier (SOA).

$R_1 = 0\%$ and $R_2 = 0\%$ over the spectral range of the gain. The parameters used in this study are shown in Table 1.

To describe the laser's dynamics, we employ the notation of Ref. [14] and write the optical field appearing in Eq. (1) as

$$\begin{aligned} E(z,t) = \mathrm{Re}\{ & E_s^+(z,t)\exp[i(\beta_s z - \omega_s t)] \\ & + E_s^-(z,t)\exp[-i(\beta_s z + \omega_s t)] \\ & + E_p^+(z,t)\exp[i(\beta_p z - \omega_p t)] \\ & + E_p^-(z,t)\exp[-i(\beta_p z + \omega_p t)] \\ & + \sum_{j=1}^{N_S}\sqrt{P_{ASE,j}^+(z,t)/A_e}\cdot\exp[i(\beta_j z - \omega_j t)] \\ & + \sum_{j=1}^{N_S}\sqrt{P_{ASE,j}^-(z,t)/A_e}\cdot\exp[-i(\beta_j z + \omega_j t)]\} \end{aligned} \tag{1}$$

where $A_e = n_g\sigma/(2Z_0)$, n_g is the group index, $\sigma = Wd/\Gamma$ is the mode cross section of the SOA, Z_0 is the characteristic impedance of vacuum, $E_s(z,t)$, $E_p(z,t)$ and $P_{ASE,j}(z,t)$ are respectively the electric fields of pump and probe lasers and ASE power at ω_j, and ω_s, ω_p, and ω_j are the angular frequencies of the pump and probe lasers and ASE respectively. The electric field of the pump laser $E_s^{\pm}(z,t)$ propagating in both forward and backward directions, can be included when reflections are provided by the facet reflectivity of the SOA.

In the slowly varying envelope approximation, we solve the set of nonlinear partial differential equations as follows. At first, the time-dependent partial differential equations that govern optical-field transmission in the device are described by

$$\begin{aligned} & \pm\frac{\partial E_s^{\pm}(z,t)}{\partial z} + \frac{1}{v_g}\frac{\partial E_s^{\pm}(z,t)}{\partial t} \\ & = \left\{-\mathrm{j}\delta_0 + \frac{1}{2}(\Gamma g_m(\lambda_s, n(z,t)) - \alpha)\right\}E_s^{\pm}(z,t) \end{aligned} \tag{2}$$

$$\begin{aligned} & \pm\frac{\partial E_p^{\pm}(z,t)}{\partial z} + \frac{1}{v_g}\frac{\partial E_p^{\pm}(z,t)}{\partial t} \\ & = \left\{-\mathrm{j}\delta_0 + \frac{1}{2}(\Gamma g_m(\lambda_p, n(z,t)) - \alpha)\right\}E_p^{\pm}(z,t) \end{aligned} \tag{3}$$

where $v_g = c/n_g$ is the group velocity, and c is the velocity of the light in vacuum. The frequency dependence or dispersion of $n(z)$ is ignored in this paper, since it becomes important only for very short pulses (1 ps or less) at the fiber lengths typically used in SOAs. $\alpha(n)$ is the material loss coefficient represented by [10]

$$\alpha(n) = K_0 + \Gamma K_1 n(z,t) \tag{4}$$

Table 1. SOA geometrical and material parameters

Symbol	Parameter	Value
L	Active region length	800 μm[10]
W	Active region width	2 μm[10]
d	Active region depth	0.4 μm[10]
Γ	Optical confinement factor	0.45[10]
α_m	Linewidth enhancement factor	3.84
N_0	Carrier density at transparency	2.0×10^{24} m^{-3}
N	Model refractive index	3.2354
η_{in}	Input coupling loss	3.0 dB[10]
η_{out}	Output coupling loss	3.0 dB[10]
R_1	Input facet reflectivity	0
R_2	Output facet reflectivity	0
K_0	Carrier-independent absorption loss coefficient	6200 m^{-1}
K_1	Carrier-dependent absorption loss coefficient	7500×10^{-24} m^2
K_g	Band-gap shrinkage coefficient	0.9×10^{-10} eVm[11]
A_{rad}	Monomolecular radiative-recombination constant	1.0×10^{7} s^{-1}
B_{rad}	Bimolecular radiative-recombination constant	5.6×10^{-16} m^3s^{-1}
A_{nrad}	Nonradiative recombination constant	3.5×10^{8} s^{-1}
B_{nrad}	Bimolecular nonradiative-recombination constant	0 m^3s^{-1}
C_{Aug}	Auger recombination constant	3.0×10^{-41} m^6s^{-1}
D_{leak}	Leakage recombination coefficient	0 $m^{13.5}s^{-1}$
y	Mole fraction of arsenide in active region	0.892[10]
a	Band-gap energy quadratic coefficient	1.35[12]
b	Band-gap energy quadratic coefficient	-0.775[12]
c	Band-gap energy quadratic coefficient	0.149[12]
m_e	Effective mass of an electron in CB	0.0452 m_0[13]
m_{hh}	Effective mass of a heavy hole in VB	0.46 m_0[13]
m_{lh}	Effective mass of a light hole in VB	0.0556 m_0[13]

where K_0 and K_1 are the carrier-independent and -dependent absorption loss coefficients respectively. K_0 represents the intrinsic material loss.

The phase parameter is given by [15]

$$\delta_0 = \beta(\lambda_k) + \frac{1}{2}\alpha_m g_m(\lambda_k, n(z,t)) \tag{5}$$

where $\beta_k = 2\pi n_g/\lambda_k$ is the wave-propagation constant of the pump or probe wave at λ_k of the pump or probe wavelength, where k is either s or p, α_m represents the linewidth enhancement factor associated with the gain change due to carrier depletion, and $g_{m,k}(\lambda_k, n(z,t))$ is the material gain.

For the consideration of the entire ASE spectrum generated in a semiconductor optical amplifier, the whole ASE spectrum is equally divided into N_s narrow spectral segments. The index j denotes a wavelength section of ASE from 1 to N_s.

$$\pm \frac{\partial P^{\pm}_{ASE,j}(z,t)}{\partial z} + \frac{1}{v_g}\frac{\partial P^{\pm}_{ASE,j}(z,t)}{\partial t} = \{\Gamma g_m(\lambda_j, n(z,t) - \alpha\} P^{\pm}_{ASE,j}(z,t) + R_{sp}(\lambda_j, n(z,t))h\nu_j \tag{6}$$

where $R_{sp}(\lambda_j, n)$ represents the spontaneous-emission noise coupled to $P^{+}_{ASE,j}(z,t)$ or $P^{-}_{ASE,j}(z,t)$

Our numerical analysis is based on a rate-equation model. The carrier density *n(z,t)* is governed by

$$\begin{aligned}\frac{\partial n(z,t)}{\partial t} = {} & \frac{I_0}{qdWL} - R(n(z,t)) \\ & - \frac{\Gamma}{hcdW}\left[\sum_{j=1}^{N_s}\lambda_j g_m(\lambda_j, n(z,t))\{P^{+}_{ASE,j}(z,t) + P^{-}_{ASE,j}(z,t)\}\right] \\ & - \frac{n_g\Gamma}{2Z_0hc}\left[\lambda_s g_m(\lambda_s, n(z,t))(E_s^{+*}E_s^{+} + E_s^{-*}E_s^{-}) \right. \\ & \left. + \lambda_p g_m(\lambda_p, n(z,t))(E_p^{+*}E_p^{+} + E_p^{-*}E_p^{-})\right]\end{aligned} \tag{7}$$

where I_0 is the bias current of the SOA. It is assumed that bias current flows only in the active region. The first term on the right-hand side of Eq. (7) represents carrier injection into the active region by the bias current I_0. These carriers are depleted according to the next three terms in Eq. (7). $R(n)$ is the recombination rate, and the material-gain spectrum of asymmetric shape is modeled as a cubic function, as in [16] and [17].

An iterative solution of Eqs. (2), (3), (6) and (7) is obtained using the fourth-order Runge-Kutta method with initial conditions $P_s(z=0,t)=P_{s0}(t)$, $P_p(z=L,t)=P_{p0}(t)$, $E_s^+(z,t=0)=0$, $E_s^-(z,t=0)=0$, $E_p^+(z,t=0)=0$, $E_p^-(z,t=0)=0$, and the following boundary conditions at the left and right ends ($z=0$ and L) of the SOA:

$$E_s^+(0,t+\Delta t)=\sqrt{R_1}\,E_s^-(0,t)+\sqrt{\eta_1(1-R_1)}\,E_{s0}(t) \quad (8)$$

$$E_s^-(L,t+\Delta t)=\sqrt{R_2}\,E_s^+(L,t) \quad (9)$$

$$E_p^+(0,t+\Delta t)=\sqrt{R_1}\,E_p^-(0,t) \quad (10)$$

$$E_p^-(L,t+\Delta t)=\sqrt{R_2}\,E_s^+(L,t)+\sqrt{\eta_2(1-R_2)}\,E_{p0}(t) \quad (11)$$

$$P_{ASE}^+(0,t+\Delta t)=\sqrt{R_1}\,P_{ASE}^-(0,t) \quad (12)$$

$$P_{ASE}^-(L,t+\Delta t)=\sqrt{R_1}\,P_{ASE}^+(L,t) \quad (13)$$

where $R_1=r_1^2$ and $R_2=r_2^2$ are the grating reflectivities. The values of the physical parameters used in our simulations are shown in Table 1. In all simulations, the probe power $E_{p0}(t)$ builds up from 0 to its maximum value with a rise time (10% to 90% of the peak) of 300 ps.

III. Simulation of the SOA

3.1. SOA simulation

To simulate the semiconductor optical amplifier, we use Eqs. (2)-(7). Including the effect of amplified spontaneous emission in the simulation, the wavelength is divided into $N_s=17$ sections, with $j=1$ to N_s. The power spectra of the output probe (O) and ASE for input probe power of 10 (red), 0 (magenta), -10 (yellow), -20 (green) and -30 dBm (blue) are shown in Fig. 2, at a probe wavelength of 1.56 μm, bias current of 80 mA, and parameter values as listed in Table 1. The copropagating (◁) and counterpropagating ASE powers (▷) are shown, according to the change in wavelength, in Figs. 2(a) and 2(b) respectively. In this figure the output probe

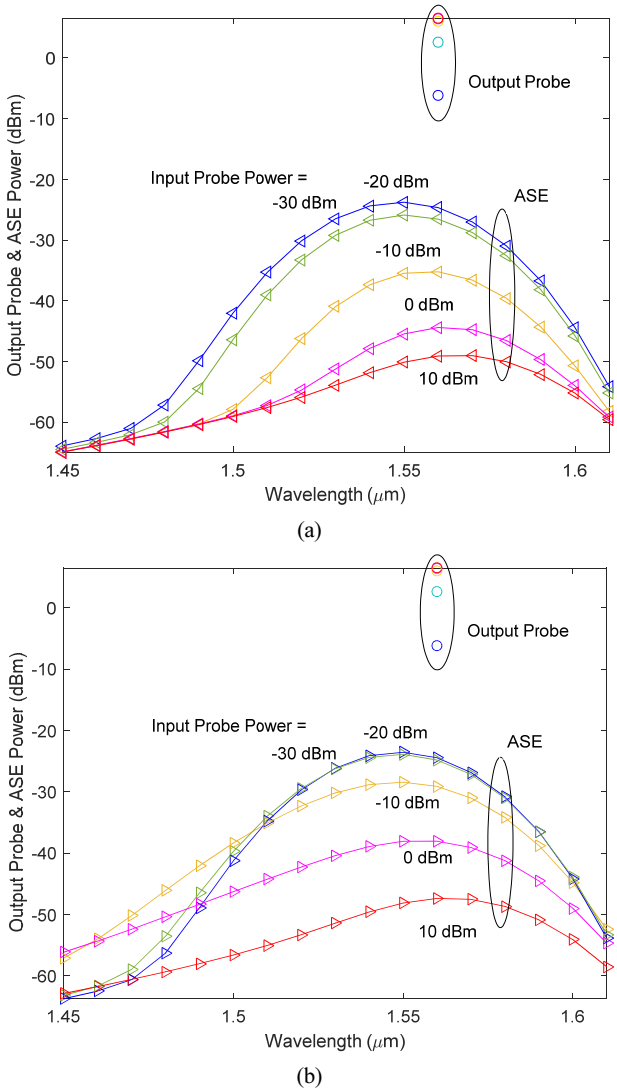

Fig. 2. Output probe power (O) and (a) copropagating (◁) and (b) counterpropagating ASE power (▷) according to the change of wavelength, when the SOA input probe power changes as 10 (red), 0 (magenta), -10 (yellow), -20 (green) and -30 dBm (blue) at a wavelength of 1.56 μm. The bias current is 80 mA, and the active region's length is 800 μm. Bandwidth resolution is 0.1 nm.

power is -6.2 dBm (Gain = 23.8 dB) and total ASE power is 5.7 dBm, at an input probe power of -30 dBm (blue). The output probe power is 6.5 dBm (Gain = 6.5 dB) and total ASE power is -9.6 dBm at an input probe power of 0 dBm (magenta). Both redshift of peak gain wavelength and gain compression are observed at high input probe power.

The output probe gain is obtained from the simulation and shown in Fig. 3(a), and copropagating and counterpropagating ASE powers are shown in Figs. 3(b) and 3(c), according to the change in input probe power from 10 to -30 dBm, at wavelengths of 1.52, 1.56, and 1.60 μm, for bias current of 80 mA and the parameter values listed in Table 1. In Fig. 3

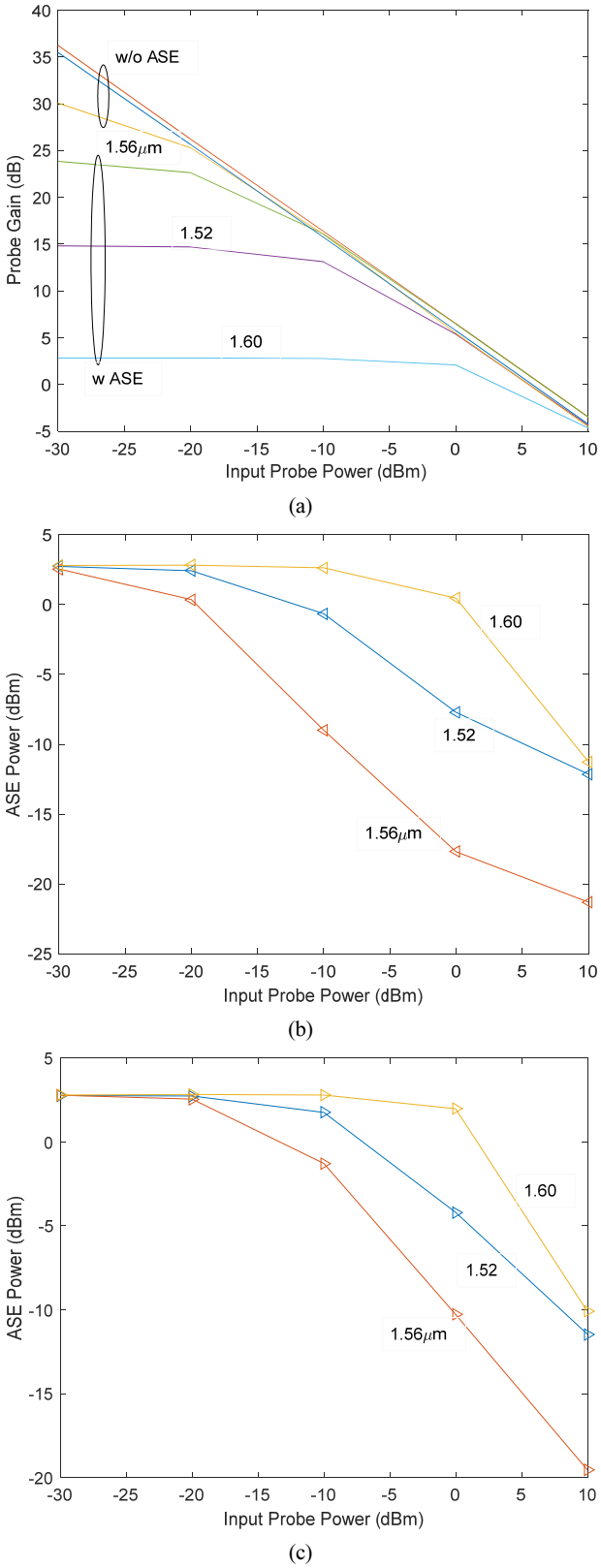

Fig. 3. (a) Probe power gain and power of (b) copropagating and (c) counterpropagating ASE power for an SOA, according to the change in probe input power from 10 to -30 dBm at probe wavelengths of 1.52, 1.56, and 1.60 μm. The bias current is 80 mA, and the length of the active region is 800 μm.

the probe power gain ranges from - 3.5 to 23.8 dB, and the copropagating ASE power from 2.5 to -21.3 dBm, by changing the input probe power from -30 to 10 dBm when the probe wavelength is 1.56 μm. In this case, gain saturation occurs at powers below -20 dBm. At other probe wavelengths, the power at which gain saturation begins is higher: -10 and 0 dBm for wavelengths of 1.52 and 1.60 μm respectively.

When ASE is not considered, all curves show almost the same output probe power for all three wavelengths at the steady state, and the gain corresponding to the input probe power is inversely proportional to the input probe power, even for different probe wavelengths. This means that the total output power is sustained at a constant value, determined by the bias current and the physical dimensions of the SOA.

Output-probe and total ASE powers of an SOA with respect to the change in wavelength are shown in Fig. 4, both with (lower three curves) and without (upper curve) ASE at an input probe power of -10 dBm. The bias current is 80 mA, and the length of the active region is 800 μm. Output probe power without and with ASE is represented by dotted and solid lines respectively. Dashed lines show total power of ASE copropagating (◁) and counterpropagating (▷) with the probe laser. As the wavelength difference from the gain's peak wavelength increased, the output probe power in the case with ASE is much smaller than without, because a huge portion of injected carriers are used in amplifying ASE. In the wavelength region with high gain, the ASE power copropagating

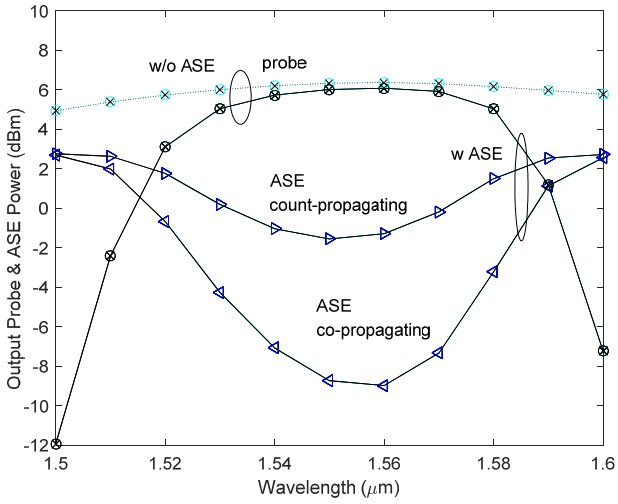

Fig. 4. Output characteristics of an SOA according to the change in probe wavelength, without ASE (upper curve) and with ASE (lower three curves), at an input probe power of -10 dBm, bias current of 80 mA, and active-region length of 800 μm. Output probe and ASE power without ASE (dotted line) and with ASE (solid line) are shown. Dashed lines show total power of ASE copropagating (◁) and counterpropagating (▷) with the probe laser.

Table 2. Output probe and ASE power (in dBm), for the cases with and without ASE. The probe power is -10 dBm

	Probe wavelength	1.52 μm	1.56 μm	1.60 μm
With ASE	Co-ASE	-0.65	-8.98	2.63
	Counter-ASE	1.76	1.29	2.79
	Probe	3.12	6.10	7.22
	Total	6.45	6.94	5.94
Without ASE	Probe	5.76	6.40	6.07

with probe laser is smaller than that counterpropagating. From Figs. 3 and 4 we can obtain the relation that the total output power from the SOA is constant, such as

$$const. = P_{ASE}^{+}(\lambda_j) + P_{ASE}^{-}(\lambda_j) + G(\lambda_j)P_{probe}(\lambda_j) \quad (14)$$

where λ_j is the wavelength of the probe and $G(\lambda_j)$ is the total gain of the probe laser at the output of the SOA. The calculated values are shown in Table 2.

3.2. Impact of gain-recovery time on ASE

A CW probe and pulsed pump laser were launched into the right and left sides of the SOA respectively. The waveforms of output probe power of the SOA for three probe wavelengths is shown in Fig. 5, for the cases without and with ASE, at an input probe power of -10 dBm, bias current of 80 mA, and active-region length of 800 μm. The gain-recovery time is defined as the time from 10% to 90% of the final power (the time between two circles in Fig. 5). The delay time is from the marker at the minimum value to the first circle. The time is determined from the energy of the pump pulse, which depends on how much carrier density is discharged by the pump pulse. As shown in Fig. 5(a), the steady-state probe powers are the almost the same as the probe wavelengths for the case without ASE, because the ASE, which has wavelength dependence, is neglected. On the other hand, in Fig. 5(b) the steady-state probe powers are different as the probe wavelength varies, for the case with ASE. This waveform of probe power is same as the waveform measured experimentally[18]. However, the impact of the ASE on gain-recovery time was not considered. Practically, the case without ASE does not exist and can be assumed only in a simulation. As a result, the gain-recovery time becomes longer as the difference between steady-state and minimum probe power is increased and the probe gain decreases.

In Fig. 6, the gain-recovery times of the SOA are shown, for probe wavelengths from 1.5 to 1.6 μm, at a probe power of -10 dBm, for the same parameters as in the simulations of

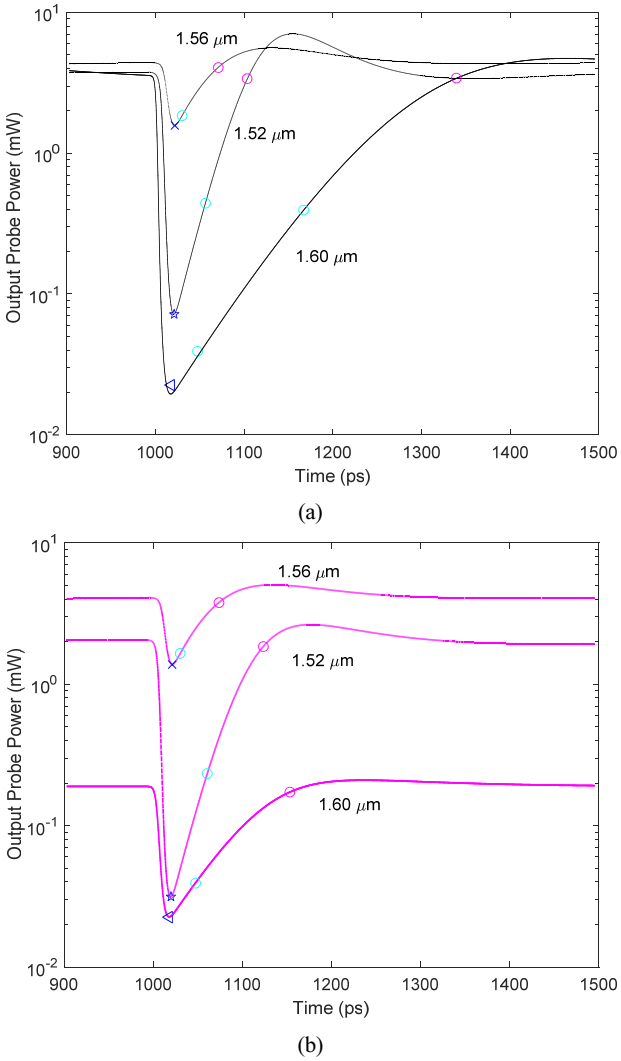

Fig. 5. Waveform of the output probe power, after applying a pump pulse of 30 fJ and pulse width of 10 ps. Gain-recovery time of the SOA for a probe power of -10 dBm according to probe wavelength, (a) without ASE and (b) with ASE.

Fig. 5. The solid and dotted lines show the cases without and with ASE respectively. Markers o and x represent the rise time and sum of delay time plus rise time of the probe power respectively. Except for the probe-wavelength range from 1.59 to 1.6 μm, the gain-recovery rise time for the case with ASE is longer than that without ASE. The figure shows that the rise time at a probe wavelength of 1.52 μm is 47 and 62 ps respectively for the cases without and with ASE, while the delay time is 35 and 41 ps. At 1.6 μm of probe wavelength, the rise times are 172 and 106 ps and the delay times are 150 and 29 ps, for the cases without and with ASE respectively. At a probe wavelength of 1.56 μm, the probe-power curves have the shortest rise times of 41 and 43 ps, and the delay times are 8.4 and 8.9 ps for the cases without and with ASE respectively.

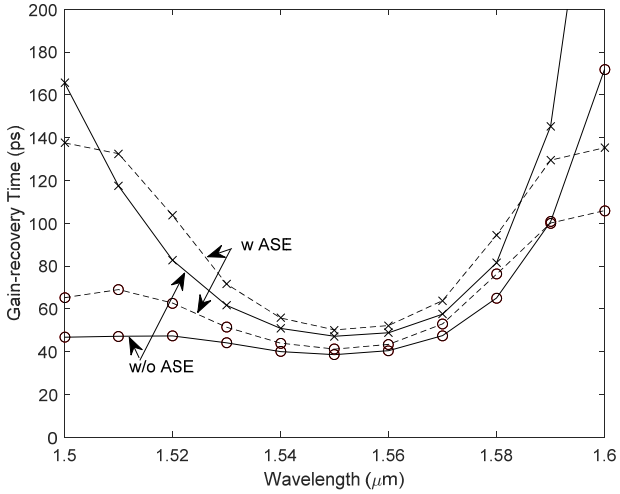

Fig. 6. The gain-recovery times of the SOA, without (solid line) and with ASE (dotted line), as the probe wavelength changes from 1.5 to 1.6 μm. Markers o and x respectively represent the rise time and the sum of delay time plus rise time of the probe power. The parameters are all the same as in Fig. 5.

IV. Conclusion

The effects of amplified spontaneous emission and CW probe wavelength on the gain-recovery time of a bulk SOA were investigated by performing numerical simulations. The gain-recovery time were obtained by determining the time evolution of the gain, carrier density, and ASE in a SOA, after propagation of a short pump pulse and CW probe of gain dynamics. In the simulations the wide-band-semiconductor model, which can be characterized by the material gain coefficient over a wide wavelength range, is used, because the gain bandwidth of a practical SOA is very wide. The ASE noise spectrum was equally divided, and the pump pulse and CW probe field propagating in both forward and backward directions were considered.

From the results of the simulations, the probe power curve has the shortest rise times of 41 and 43 ps, and the delay times are 8.4 and 8.9 ps, at a probe wavelength of 1.56 μm, for the cases without and with ASE respectively. As the probe wavelength increases, the gain-recovery time also increases. The CW probe power with -10 dBm and pump pulse of 30 fJ with pulse width of 10 ps counterpropagate with respect to each other. The steady-state probe powers are almost the same for all probe wavelengths, without ASE, because the wavelength dependence of the ASE was neglected. On the other hand, the steady-state probe powers were found to be different for various probe wavelengths, with ASE. The time is determined from the energy of the pump pulse, which depends on how much carrier density is discharged by the pump pulse. As a result, the gain-recovery time becomes longer as the difference between steady-state and minimum probe power increases, and probe gain decreases.

Acknowledgement

This research was supported by the Hoseo University research grant in 2016.

References

1. K. Stubkjær, “Semiconductor optical amplifier-based all-optical gates for high-speed optical processing,” IEEE J. Sel. Topics Quantum Electron. **6**, 1428-1435 (2000).
2. F. Ginovart, J. C. Simon, and I. Valiente, “Gain recovery dynamics in semiconductor optical amplifier,” Opt. Commun. **199**, 111-115 (2001).
3. R. J. Manning and D. A. O. Davies, “Three-wavelength device for all-optical signal processing,” Opt. Lett. **19**, 889-891 (1994).
4. R. J. Manning, D. A. O. Davies, and J. K. Lucek, “Recovery rates in semiconductor laser amplifiers: optical and electrical bias dependencies,” Electron. Lett. **30**, 1233-1235 (1994).
5. J. L. Pleumeekers, M. Kauer, K. Dreyer, C. Burrus, A. G. Dentai, S. Shunk, J. Leuthold, and C. H. Joyner, “Acceleration of gain recovery in semiconductor optical amplifiers by optical injection near transparency wavelength,” IEEE Photon. Technol. Lett. **14**, 12-14 (2002).
6. M. A. Dupertuis, J. L. Pleumeekers, T. P. Hessler, P. E. Selbmann, B. Deveaud, B. Dagens, and J. Y. Emery, “Extremely fast high-gain and low current SOA by optical speed-up at transparency,” IEEE Photon. Technol. Lett. **12**, 1453-1455 (2000).
7. H. Wei, H. Dexiu, S. Junqiang, and L. Deming, “Numerical simulation of recovery enhancement by a CW pump light in semiconductor optical amplifiers,” Opt. Commun. **214**, 335-341 (2002).
8. X. Li, M. J. Adams, D. Alexandropoulos, and I. F. Lealman, “Gain recovery in semiconductor optical amplifiers,” Opt. Commun. **281**, 3466-3470 (2008).
9. M. J. Connelly, “Wideband semiconductor optical amplifier steadystate numerical model,” IEEE J. Quantum Electron. **37**, 439-447 (2001).
10. C. Deguet, D. Delprat, G. Crouzel, N. J. Traynor, P. Maigne, T. Pearsal, C. Lerminiaux, N. Andreakis, C. Caneau, F. Favire, R. Bhat, and C. E. Zah, “Homogeneous buried ridge stripe semiconductor optical amplifier with near polarization independence,” in *Proc. Eur. Conf. Optical Communications* (1999).
11. S. Adachi, *GaAs and Related Materials* (Singapore: World Scientific, 1994).
12. S. Adachi, *Physical Properties of III-IV Semiconductor Compounds* (New York: Wiley, 1992).

13. S. L. Chuang, *Physics of Optoelectronic Devices* (New York: Wiley Interscience, 1995).
14. G. P. Agrawal, *Nonlinear Fiber Optics*, 4th ed. (Academic, 2007).
15. D. A. Marcuse, "Computer model of an injection laser amplifier," IEEE J. Quantum Electron. **19**, 63-73 (1983).
16. G. P. Agrawal and N. K. Dutta, *Semiconductor Lasers* (Van Nostrand Reinhold, New York, 1993).
17. S. Toshiaki, *Semiconductor Laser Fundamentals* (Marcel Dekker, Inc., New York, 2004).
18. A. Sharaiha, M. Amaya, and J. Le Bihan, "Improvement of semiconductor optical amplifier dynamic behaviour by assist light injection," in *Proc. London Communications Symposium (LCS2005)* (London, UK, September 8-9, 2005).